Journal of Physics: Conference Series

Preservation and Reproduction of an Ancient Human Humerus through X-ray Microscopy and 3D Printing

To cite this article: Flavio Cognigni *et al* 2023 *J. Phys.: Conf. Ser.* **2579** 012011

Preservation and Reproduction of an Ancient Human Humerus through X-ray Microscopy and 3D Printing

Flavio Cognigni[1*], Valentina Alemanno[1], Luciano Fattore[2], Eleonora Stornelli[1], Francesco Genchi[3], Marco Rossi[1]

[1] Department of Basic and Applied Sciences for Engineering (SBAI), University of Rome LA SAPIENZA, 00185, Italy
[2] Saperi&co research and services center, University of Rome LA SAPIENZA, 00185, Italy
[3] Department Italian Institute of Oriental Studies (ISO), University of Rome LA SAPIENZA, 00185, Italy

*Corresponding author e-mail: flavio.cognigni@uniroma1.it

Abstract. The combination of X-ray Microscopy (XRM) and three-dimensional virtual reconstruction has enabled the digitization and restoration of broken artifacts. By scanning, acquiring, and virtually stitching together the 3D reconstructions of individual broken pieces, damaged relics can be visualized as if they were intact objects. These virtually reconstructed samples can then be reproduced as physical copies through 3D printing, allowing for the sharing of rare findings in museum exhibits worldwide so that printed copies can be displayed for public exposure, while the original pieces remain preserved. This paper aims to demonstrate the application of these reconstruction principles to an artificially modified human humerus belonging to the II–I millennium BC. The humerus was bent into the shape of a serpent for ritual purposes related to the ancient "Snake Cult", which was widespread in the Persian Gulf area during the Iron Age. Following the scanning and software elaboration processes, the pieces were printed in Polylactic Acid (PLA) as a single object and made available to the public, thus giving new life to a unique piece of history.

1. Introduction

As we enter the Digital Age, it is becoming increasingly common to digitize rare artifacts, which allows for their preservation and analysis without causing any associated damage [1]. Moreover, by acquiring three-dimensional images of individual broken pieces of an artifact, it is possible to stitch them together and to reconstruct the object as a whole [2]. These reconstructed copies can then be distributed to museums around the world for public display instead of the original pieces, whenever these are too frail to exhibit [3] [4] [5]. This approach was successfully applied to a unique archeological find: a human humerus discovered at the LCG2 complex at Dibbā (Musandam, Oman, II–I millennium BC) which had been bent to resemble the shape of a serpent [6]. The find is believed to have been used as a ceremonial object related to the "Snake Cult" that wase widespread in the Persian Gulf during the Iron Age [7] [8] [9]. The process that was employed for bending the specimen is not investigated in this paper, as it will be part of further studies. In Fig. 1 the textured 3D model render obtained from a photogrammetric survey of the humerus in situ during the excavation campaign of 2014-2015 is reported. Digital images of the sample were acquired via X-ray Microscopy (XRM).

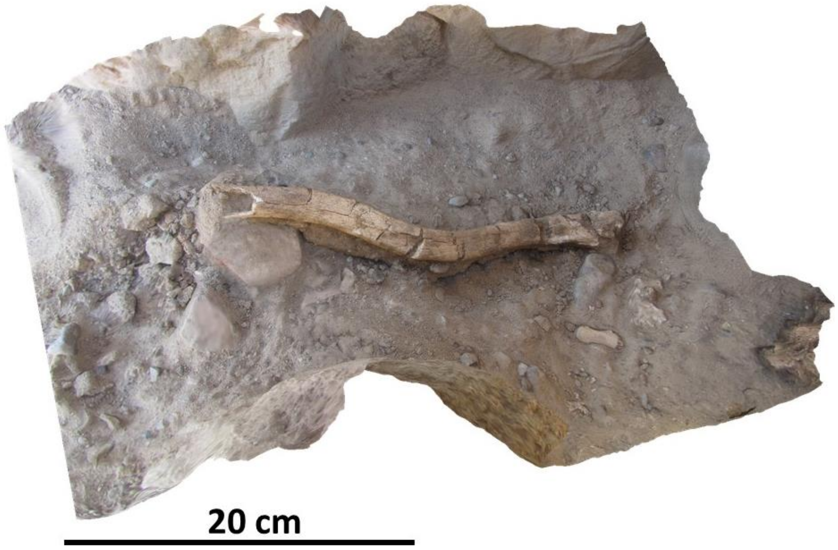

Fig. 1 -Textured 3D model render obtained from a photogrammetry survey. The humerus was found in the LCG2 complex at Dibbā (Musandam, Oman, II–I millennium BC) and had been bent to resemble the shape of a serpent.

X-ray Microscopy (XRM) is a characterization technique that allows the three-dimensional investigation of internal features of specimens in a non-destructive way [10] [11] [12] [13]. XRM has been involved in wide range of applications such as aerospace [14, 15], energy materials research [16, 17, 18], electronics and semiconductors [19, 20], cultural heritage [21, 22, 23, 24], biomedical engineering [25, 26], and biology [27]. The contrast obtained in the final image strongly depends on the X-ray absorption phenomenon that occurs along the X-ray beam path $\boldsymbol{L}$ (in m) inside the sample which is function of the attenuation coefficient value $\boldsymbol{\mu(x)}$ (in m^{-1}) in a certain position $\boldsymbol{x}$ (in m) along the path inside the specimen and depends on the intensity of the X-ray beam before entering the sample $\boldsymbol{I_0}$ (in Watt). The transmitted X-ray beam intensity $\boldsymbol{I(L)}$ which is responsible of the image formation is expressed by the Beer-Lambert law (Eq. 1):

$$I(L) = I_0 e^{-\int_0^L \mu(x) dx} \tag{1}$$

The experimental setup of an XRM investigation consists of an X-rays source, a detector that collects the transmitted X-ray beam [a charged-coupled device (CCD) or a complementary metal-oxide semiconductor (CMOS), and a sample chamber located between these two components where the sample holder is positioned to ensure its mechanical stability and rotation. Even though traditional scanning techniques that rely on visible structured light may be suitable for 3D printing or reconstruction they become ineffective for objects with concealed or internal features. In this case, the ability of XRM to non-destructively investigate archaeological artefacts is crucial to provide a faithful reconstruction of the interior and exterior of the object.

2. Materials & Methods

2.1 Sample description

The human humerus discovered at the LCG2 complex at Dibbā (Musandam, Oman, II–I millennium BC) and had been bent to resemble the shape of a serpent. We believe that the specimen have been used as a ceremonial object related to the "Snake Cult" that was widespread in the Persian Gulf during the Iron Age [7] [8] [9]. The shape of the humerus must have been modified when its organic component had not yet been lost, because the inorganic component alone does not provide sufficient elasticity to the bone.

2.2 X-ray Microscopy (XRM) investigation and 3D reconstruction

XRM analysis was performed using a ZEISS Xradia Versa 610 X-ray microscope available at the Research Centre on Nanotechnology Applied to Engineering (CNIS) of Sapienza University of Rome that is part of the open infrastructure for Advanced Tomography and Microscopies (ATOM). The bone specimen was broken into 5 pieces, as shown in Fig. 2a, although some fragments may have been lost. Each of these five pieces was placed in a separate polystyrene sample holder, numbered from 1 to 5 in descending order of size, as shown in Fig. 2b. Subsequently, a distinct XRM scan was performed for each of these samples. The voltage and power of the X-ray source were 80 kV and 10 W for all the samples except for piece n. 5, the smallest one, in which they were 60 kV and 5 W respectively. For all samples, a bin 2 and a 0.4x objective were set, while the exposure time was 2.5 s to optimize the signal collection. The total scan time for all the samples ranged from 2 to 7 hours. To overcome the limitations of the limited Field Of View (FOV), pieces n. 1 and n. 2 required the use of the vertical stitch scan mode. Once chosen a starting and an ending point along the vertical y-axis of the object, acquisition software *Scout-and-Scan control system* (V. 16.1.14271.44713) performs an automatic separation of the object in several sub-volumes which are then stitched together at the end of the reconstruction process based on the Feldkamp-Davis-Kress (FDK) algorithm.

Fig. 2 - Humerus pieces numbered 1 to 5.

2.3 Image Processing

The reconstructed 3D datasets were imported into Dragonfly Pro (V. 2022.1 Build 1259) [28] software for segmentation, alignment, and mesh export.

2.4 3D printing

Rarely meshes coming out from whatever scanning technology are ready for 3D printing. Noise, missing parts, and meshing defects need to be removed to have a *watertight model*. Several softwares have been used to reach this goal. Meshlab [29] filtering functions were used to roughly clean defects, Rhinoceros [30] to rearrange some triangles, Zbrush [31] and Blender [32] to smooth spikes or to reconstruct regions that clearly were incorrect. This workflow has been used to minimize the arbitrary modification of original shape of the samples. To align correctly the meshes obtained from XRM scans they have been imported into CloudCompare [33] with the 3D model from the photogrammetric survey. Using the latter as reference model, several roto-translations have been applied to the models to improve their alignment. The result of such assembling has been sliced with the software PrusaSlicer [34] with variable (0,2÷0,05) mm thickness and printed in PLA, with a Prusa MK3S+, as a whole object sectioned in two halves kept together by a magnet, making it possible to open the bone and observe its inner structure.

3. Results and Discussions

Upon examination, it was found that the humerus was broken in ancient, after decomposition of organic portion of the bone due to the combined action of the dry climate, periodic flooding, the weight of the soil and other taphonomic influences on the burial, thus resulting the splitting into multiple parts as we have received for analysis, as illustrated in Fig. 2a. Some of these pieces were presumed to have been lost due to the reasons discussed in the following. For the purposes of this study, we scanned the five largest and most consistent pieces via XRM, which are shown in Fig. 2b. The other fragments were too small to be of significance for the overall reconstruction objective. Of the five pieces, we were able to align three that were most consistent with one another, corresponding to pieces n.1, 2 and 4. XRM results for piece n. 1 are presented in 3D (left) and 2D slices on the XZ plane (right) in Fig. 3. Three planes (green, red, and blue) were selected along the y-axis of the specimen to visualize single slices on the XZ plane. The scans revealed that the humerus was covered with dirt, rocks, and soil residue, some of which was trapped within the bone's internal cavity. The entire volume of the cavity was filled with dirt, rocks, and soil debris. The humerus was characterized by numerous fractures and voids. The lower part of piece n. 1 had a particularly high density of damage, including fractures, cracks, and voids, as highlighted by the blue plane in Fig. 3. This information suggests that the sample is particularly delicate, and any manipulation could result in its destruction. X-ray technology can non-destructively penetrate materials, allowing hidden or inaccessible features to be visualized. This contrasts with traditional techniques that rely on visible structured light, which may be suitable for 3D printing or reconstruction but are ineffective for objects with concealed or internal features. To enable proper reconstruction and 3D printing, the dirt and soil residues must be removed from the sample. However, removing these substances from a fragile sample could damage the object. Thus, the recommended approach is to use 3D modeling to remove these phases. The stack of projections was segmented via histogram-based thresholding to separate the bone phase from the soil.

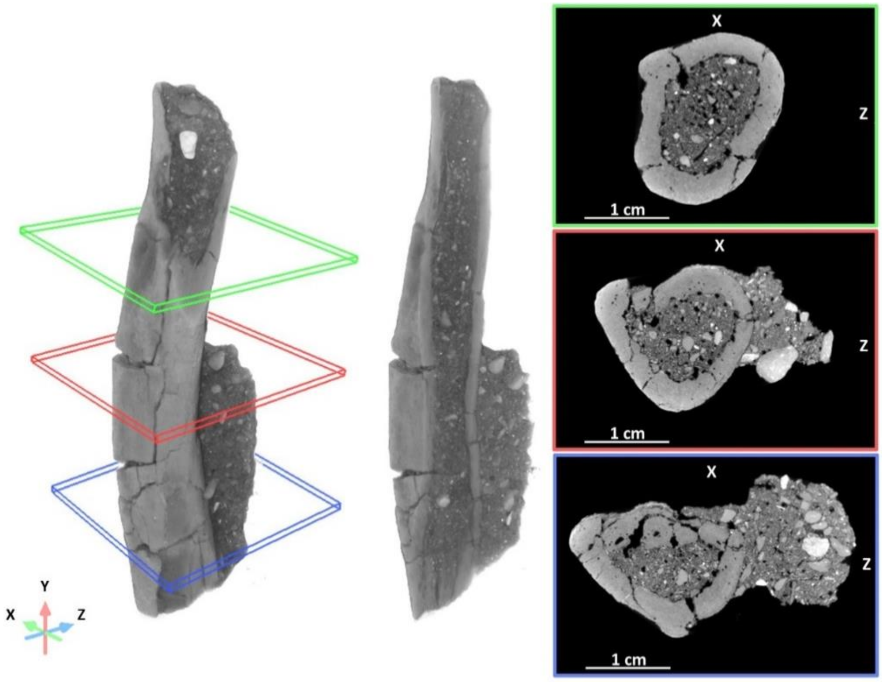

Fig. 3 – The 3D reconstruction of the humerus (piece n. 1) and the digital cross-section (left) reveal that dirt, rocks and some products of the soil are attached to the surface of the humerus and trapped inside its internal cavity. Three planes (green, red, and blue) were selected along the y-axis to visualize single slices on the XZ plane (right). Several fractures and voids can be distinguished all over the humerus revealing a critical fragility of the object.

The segmentation process involved the following protocol. Firstly, a region of interest (ROI) was created for each bone piece containing all the phases present in the object, which were labelled as containing both bone, dirt and products of the soil. Next, all pixels clearly interpretable as dirt were isolated and included in a separate ROI labelled as soil. Subsequently, using Boolean operations, we subtracted the ROI containing exclusively soil pixels from the one marking both bone and dirt pixels. This resulted in an approximately isolated ROI primarily consisting of pixels belonging to the bone structure. The newly obtained ROI was then polished using a spherical brush-shaped painting tool to manually remove any marked pixels that still belonged to the dirt phase. Once the polishing process was completed, the ROIs were refined using a *process islands* function to remove small groups of pixels interpretable as noise. Then, morphological operations were applied, meaning the ROI was subjected to subsequent processes of *closing* to remove any small holes in the object. The results obtained from this dedicated image processing workflow are reported in Fig. 4. 3D models and digital cross sections witness the successful operation of dirt, rocks, and soil products removal from the internal cavity of the piece and from its surfaces. This allowed the possibility to appreciate external and internal surfaces of the bone specimen avoiding the need to perform any sort of manipulation over the delicate sample, hence ensuring its preservation. Piece n.1, that was already described in the first part of the section, is depicted in violet in Fig. 4a. Pieces n.2 and n.4, depicted in green and red respectively in Fig. 4b and Fig. 4c, show a similar condition where considerable amounts of dirt and products of the soil are distributed over their surfaces and in the internal cavity. Observing the digital cross-sections of the pieces after the removal of dirt and soil product one can notice that the bone sample preserved only the cortical region whilst the porous trabecula was subjected to erosion over time, hence it cannot be studied and reproduced. The processed XRM datasets were aligned and stitched together using the *Displace* function of Dragonfly Pro (Version 2022.1 Build 1259) from Object Research Systems (ORS). The importance of documenting as best we can each phase of archaeological research comes out in this circumstance if we consider that the alignment step was guided by the information collected with the photogrammetric survey (Fig. 1). We were able to align and stitch three out of the five parts, corresponding to pieces n.1, 2 and 4 (see Fig. 2b), since none of the combinations of the five fragments were consistent enough. Therefore, we presume that some of the original components of the ancient humerus were lost or destroyed during the excavation and transportation process.

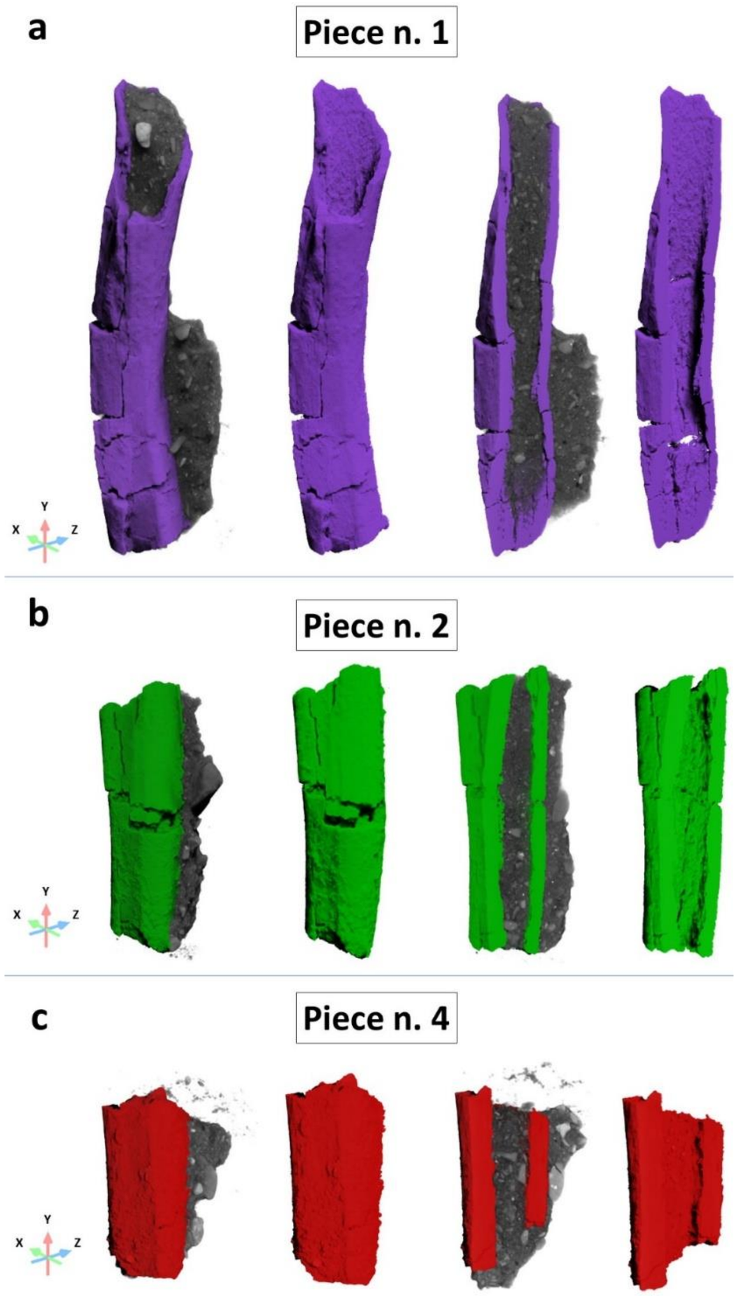

Fig. 4 - To enable proper reconstruction and 3D printing, the dirt and soil residues must be removed from the pieces composing the sample. (a) 3D models and digital cross sections of piece n.1, depicted in violet, witness the successful operation of dirt, rocks, and soil products removal from the internal cavity of the piece and from its surfaces. (b) Piece n.2 and (c) piece n.4, depicted in green and red respectively show a similar condition where considerable amounts of dirt and products of the soil are distributed over their surfaces and in the internal cavity that were successfully removed.

Based on the alignment of the three bone pieces, shown in Fig. 5, we were able to create a three-dimensional reconstruction of the bone specimen using 3D printing technology, as shown in Fig. 6. The object was printed in PLA, with a Prusa MK3S+, as a whole object, as shown in Fig. 6a, sectioned in two halves kept together by a magnet, making it possible to open the bone and observe its inner structure, as depicted in Fig. 6b.

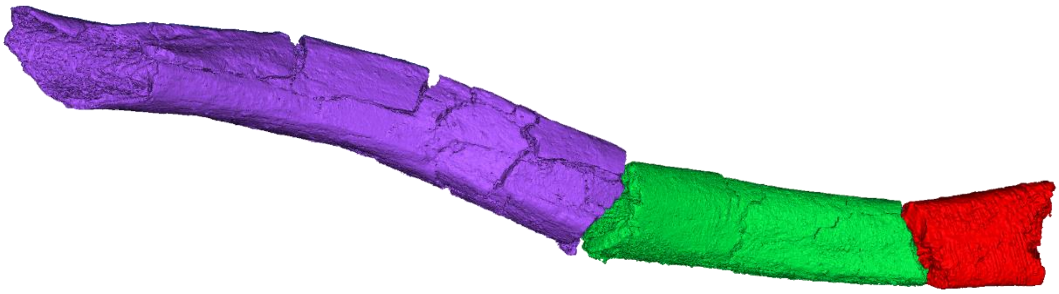

Fig. 5 - The alignment step of the meshes (.STL) representing pieces n.1, 2 and 4 was guided by the information provided by the photogrammetry data. None of the combinations of the five fragments were consistent enough. Therefore, we presume that some of the original components of the ancient humerus were lost or destroyed during the excavation and transportation process.

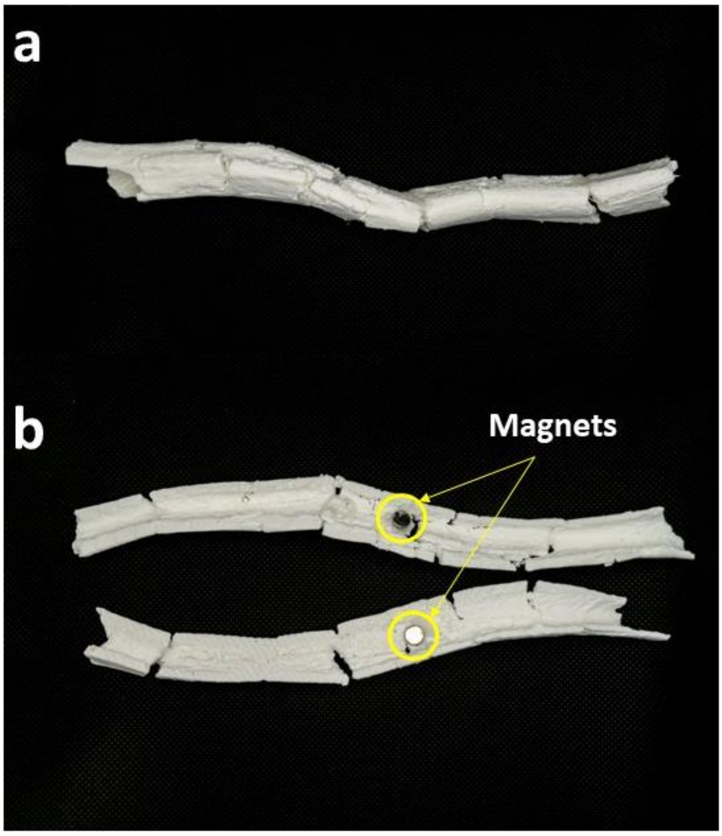

Fig. 6 - Based on the digital alignment of the three bone pieces, the reconstruction of the human humerus was 3D printed. In (a) the reconstructed bone is shown in its entirety whilst in (b) the same object is opened in two separate parts that can be joined using a magnet glued to both parts. This allows us to show internal features and hidden details of the internal cavity of the ancient humerus.

4. Conclusions

In this work we demonstrated the successful application of reconstruction principles to an artificially modified human humerus belonging to the II–I millennium BC. The bone specimen was bent into the shape of a serpent for ritual purposes related to the ancient "Snake Cult" which was widespread in the Persian Gulf area during the Iron Age. The combination of X-ray Microscopy (XRM), dedicated image processing workflow and three-dimensional virtual reconstruction as well as 3D printing has been shown to be a powerful tool for the digitization and restoration of damaged artifacts which present hidden features that are not accessible with other techniques [35] [36] [37]. By scanning and virtually stitching together 3D reconstructions of individual broken pieces, damaged relics can be visualized as if they were intact objects. These virtually reconstructed samples were reproduced as physical copies through 3D printing, allowing for the sharing of rare findings in museum exhibits worldwide.

5. Acknowledgements

This research has been realized with the financial support of the project ATOM (Advanced Tomography and Microscopies), granted by Lazio Region (call "Open infrastructures for Research").

References

[1] M. Pieraccini, G. Guidi and C. Atzeni, "3D digitizing of cultural heritage," *Journal of Cultural Heritage,* vol. II, pp. 63-70, 2001.

[2] S. D. Laicock, G. D. Bell, N. Corps, D. B. Mortimore, G. Cox, S. May and I. Finkel, "Using a Combination of Micro–Computed Tomography, CAD and 3D Printing Techniques to Reconstruct Incomplete 19th-Century Cantonese Chess Pieces," *ACM Journal on Computing and Cultural Heritage,* vol. VII, no. 4, pp. 1-6, 2015.

[3] M. Neumüller, A. Reichinger, F. Rist and C. Kern, 3D Printing for Cultural Heritage: Preservation, Accessibility, Research and Education, Springer-Verlag Berlin Heidelberg, 2014, pp. 119-134.

[4] A. Tamberino, S. McAvoy, M. Howland, B. Liss, K. Bennallack and T. Levy, *3D Printing for Cultural Heritage Preservation and Education,* 2017.

[5] C. Balletti, M. Ballarin and F. Guerra, "3D printing: State of the art and future perspectives," *Journal of Cultural Heritage,* vol. XXVI, pp. 172-182, 2017.

[6] L. Fattore, A. Nava, F. Genchi, D. Mancinelli and E. Maini, L'area sacra di Daba (Musandam, Oman, II-I millennio a.C.).I morti oltre la morte. L'analisi tafonomica e l'interpretazione dei processi culturali e naturali sulle ossa di LCG2, 2015, pp. 375-385.

[7] A. Benoist, "An Iron Age II snake cult in the Oman peninsula: evidence from Bithnah (Emirate of Fujairah)," *Arabian archeology and epigraphy,* vol. VIII, no. 1, pp. 34-54, 2007.

[8] G. Gernez, M. Jean and A. Benoist, "The discovery of a new Iron Age ritual complex in central Oman: recent excavations near Ādam," *Proceedings of the Seminar for Arabian Studies,* no. 47, pp. 101-117, 2017.

[9] M. Jean, M. P. Pellegrino and G. Gernez, "New evidence of Iron Age ritual practices in central Oman: 2017 excavations in Muḍmār East, near Āda," *Proceedings of the Seminar for Arabian Studies,* no. 48, pp. 125-141, 2018.

[10] F. Cognigni, S. Dinarelli, M. Girasole, G. Longo, G. Fabi and M. Rossi, "3D X-ray Microscopy (XRM) investigation of exogenous materials inside mussels' organs," *IOP Conference Series: Materials Science and Engineering,* no. 1265, November 2022.

[11] R. Abel, S. Parfitt, N. Ashton, S. G. Lewis, B. Scott and C. Stringer, "Digital preservation and dissemination of ancient lithic technology with modern micro-CT," *Computers & Graphics,* vol. XXXV, no. 4, pp. 878-884, 2011.

[12] M. P. Morigi, F. Casali, M. Bettuzzi, R. Brancaccio and V. D'Errico, "Application of X-ray Computed Tomography to Cultural Heritage diagnostics," *Applied Physics A,* vol. 100, pp. 653-661, 2010.

[13] F. G. Bossema, S. B. Coban, A. Kostenko, P. Van Duin, J. Dorscheid, I. Garachon, E. Hermens, R. Van Liere and K. Joost Batenburg, "Integrating expert feedback on the spot in a time-efficient explorative CT scanning workflow for cultural heritage objects," vol. 10, pp. 38-47, 2021.

[14] A. Du Plessis and P. Rossouw, "X-ray computed tomography of a titanium aerospace investment casting," *Case Studies in Nondestructive Testing and Evaluation,* vol. 3, pp. 21-26, 2015.

[15] P. Chowdhury, H. Sehitoglu and R. Rateick, "Damage tolerance of carbon-carbon composites in aerospace application," *Carbon,* no. 126, 2018.

[16] F. Cognigni, M. Pasquali, P. P. Prosini, C. Paoletti, A. Aurora, F. A. Scaramuzzo and M. Rossi, "X-Ray Microscopy: A Non-Destructive Multi-Scale Imaging to Study the Inner Workings of Batteries," *ChemElectroChem,* 2023.

[17] D. Dini, F. Cognigni, D. Passeri, A. F. Scaramuzzo, M. Pasquali and M. Rossi, "Review—Multiscale Characterization of Li-Ion Batteries through the Combined Use of Atomic Force Microscopy and X-ray Microscopy and Considerations for a Correlative Analysis of the Reviewed Data," *Journal of The Electrochemical Society,* vol. 168, no. 126522, 2021.

[18] P. Trogadas, O. O. Taiwo, B. Tjaden, T. P. Neville, S. Yun, J. Parrondo, V. Ramani, M. O. Coppens, D. J. L. Brett and P. R. Shearing, "X-ray micro-tomography as a diagnostic tool for the electrode degradation in vanadium redox flow batteries," *Electrochemistry Communications,* vol. 48, pp. 155-159, 2014.

[19] C. Hartfield, C. Schmidt, A. Gu and S. T. Kelly, "From PCB to BEOL: 3D X-Ray Microscopy for Advanced Semiconductor Packaging," in *IEEE International Symposium on the Physical and Failure Analysis of Integrated Circuits (IPFA)*, 2018.

[20] S. M. Zulkifli, B. Zee, W. Qiu and A. Gu, "High-res 3D X-ray microscopy for non-destructive failure analysis of chip-to-chip micro-bump interconnects in stacked die packages," in *IEEE 24th International Symposium on the Physical and Failure Analysis of Integrated Circuits (IPFA)*, 2017.

[21] M. Bernabale, F. Cognigni, F. Mura, L. Nigro, D. Montanari, M. Rossi and C. De Vito, "3D imaging of micro-segregation and corrosion behavior of alloying elements in archaelogical artefacts from Motya (Sicily, Italy)," *Corrosion Science,* vol. 211, no. 110900, 2023.

[22] M. Bernabale, F. Cognigni, L. Nigro, M. Rossi, T. De Caro and C. De Vito, "A comprehensive strategy for exploring corrosion in iron-based artefacts through advanced Multiscale X-ray Microscopy," *Scientific Reports,* vol. 12, no. 6125, 2022.

[23] M. Bernabale, F. Cognigni, L. Nigro, M. Rossi and C. De Vito, "Conventional and advanced techniques for archaelogical diagnostic of iron artefacts," in *2022 IMEKO TC-4 International COnference on Metrology for Archaeology and Cultural Heritage University of Calabria,* Cosenza, 2022.

[24] V. Gonzalez, M. Cotte, F. Vanmeert, W. De Nolf and K. Janssens, "X-ray Diffraction Mapping for Cultural Heritage Science: a Review of Experimental Configurations and Applications," *Chemistry - A European Journal,* vol. 26, no. 8, pp. 1703-1719, 2019.

[25] M. Razavi, Y. Qiao and A. S. Thakor, "Three-dimensional cryogels for biomedical applications," *Journal of Biomedical Materials Research,* vol. 107, no. 12, pp. 2736-2755, 2019.

[26] E. O. Bachtiar, O. Erol, M. Millrod, R. Tao, D. H. Gracias, L. H. Romer and S. H. Kang, "3D printing and characterization of a soft and biostable elastomer with high flexibility and strength for biomedical applications," *Journal of the Mechanical Behavior of Biomedical Materials,* vol. 104, 2020.

[27] F. Cognigni, S. Dinarelli, M. Girasole, G. Longo, G. Fabi and M. Rossi, "3D X-ray Microscopy (XRM) investigation of exogenous materials inside mussels' organs," in *NanoInnovation 2021*, 2022.

[28] "Dragonfly," [Online]. Available: https://www.theobjects.com/dragonfly/index.html.

[29] Visual Computing Lab ISTI-CNR, "MeshLab," [Online]. Available: https://www.meshlab.net/.

[30] Robert McNeel & Associates, "Rhinoceros," [Online]. Available: https://www.rhino3d.com/.

[31] Maxon Computer GMBH, "ZBrush," [Online]. Available: https://pixologic.com/.

[32] Blender, "Blender," [Online]. Available: https://www.blender.org/.

[33] CloudCompare, "CloudCompare," [Online]. Available: https://www.danielgm.net/cc/.

[34] Prusa Research, "PrusaSlicer," [Online]. Available: https://www.prusa3d.com/it/pagina/prusaslicer_424/.

[35] E. M. Withers and P. J., "Quantitative X-ray tomography," *International Materials Reviews,* vol. 59, no. 1, pp. 1-43, 2014.

[36] B. Bertoglio, S. Corradin, A. Cappella, D. Mazzarelli, L. Biehler-Gomez, C. Messina, G. Pozzi, L. M. Sconfienza, F. Sardanelli, C. Sforza, D. De Angelis and C. Cattaneo, "Pitfalls of Computed Tomography 3D Reconstruction Models in Cranial Nonmetric Analysis," *Journal of Forensic Sciences,* vol. 65, no. 6, 2020.

[37] M. Holt, R. Harder, R. Winarski and V. Rose, "Nanoscale Hard X-Ray Microscopy Methods for Materials Studies," *Annual Review of Materials Research*, vol. 43, no. 1, pp. 183-211, 2013.